Optical trapping of coated microspheres

Volker Bormuth,[1,†] **Anita Jannasch,**[1,†] **Marcel Ander,**[2] **Carlos M. van Kats,**[3] **Alfons van Blaaderen,**[3] **Jonathon Howard,** [1] **and Erik Schäffer**[2,*]

[1]*Max Planck Institute of Molecular Cell Biology and Genetics, Pfotenhauerstraße 108, 01307 Dresden, Germany*
[2]*Nanomechanics Group, Biotechnology Center, TU Dresden, Tatzberg 47-51, 01307 Dresden, Germany*
[3]*Soft Condensed Matter, Debye Institute for Nanomaterials Science, Utrecht University, Princetonplein 5, 3584 CC Utrecht, The Netherlands*
[†] *These authors contributed equally to this work.*

[*]*Corresponding author: Erik.Schaeffer@biotec.tu-dresden.de*

Abstract: In an optical trap, micron-sized dielectric particles are held by a tightly focused laser beam. The optical force on the particle is composed of an attractive gradient force and a destabilizing scattering force. We hypothesized that using anti-reflection-coated microspheres would reduce scattering and lead to stronger trapping. We found that homogeneous silica and polystyrene microspheres had a sharp maximum trap stiffness at a diameter of around 800 nm—the trapping laser wavelength in water—and that a silica coating on a polystyrene microsphere was a substantial improvement for larger diameters. In addition, we noticed that homogeneous spheres of a correct size demonstrated anti-reflective properties. Our results quantitatively agreed with Mie scattering calculations and serve as a proof of principle. We used a DNA stretching experiment to confirm the large linear range in detection and force of the coated microspheres and performed a high-force motor protein assay. These measurements show that the surfaces of the coated microspheres are compatible with biophysical assays.

OCIS codes: (120.5820) Scattering measurements; (140.7010) Laser trapping; (160.2710) Inhomogeneous optical media; (260.3160) Interference; (260.5430) Polarization; (290.4020) Mie theory; (310.0310) Thin films; (350.4855) Optical tweezers or optical manipulation; (170.0170) Medical optics and biotechnology

References and links

1. K. Svoboda and S. M. Block, "Biological Applications of Optical Forces," Annu. Rev. Biophys. Biomol. Struct. **23**, 247–285 (1994).
2. A. Ashkin, "Optical trapping and manipulation of neutral particles using lasers," Proc. Natl. Acad. Sci. U. S. A. **94**, 4853–4860 (1997).
3. D. G. Grier, "Optical tweezers in colloid and interface science," Curr. Opin. Colloid Interface Sci. **2**, 264–270 (1997).
4. A. D. Mehta, M. Rief, J. A. Spudich, D. A. Smith, and R. M. Simmons, "Single-molecule biomechanics with optical methods," Science **283**, 1689–1695 (1999).
5. D. G. Grier, "A revolution in optical manipulation," Nature **424**, 810–816 (2003).
6. C. Bustamante, Z. Bryant, and S. B. Smith, "Ten years of tension: single-molecule DNA mechanics," Nature **421**, 423–427 (2003).
7. K. Neuman and S. Block, "Optical Trapping," Rev. Sci. Instrum. **75**, 2787–2809 (2004).

#96526 - $15.00 USD Received 27 May 2008; revised 24 Jul 2008; accepted 3 Aug 2008; published 22 Aug 2008

8. C. Graf, D. L. J. Vossen, A. Imhof, and A. van Blaaderen, "A general method to coat colloidal particles with silica," Langmuir **19**, 6693–6700 (2003).
9. S. F. Tolić-Nørrelykke, E. Schäffer, J. Howard, F. S. Pavone, F. Jülicher, and H. Flyvbjerg, "Calibration of optical tweezers with positional detection in the back focal plane," Rev. Sci. Instrum. **77**, 103101 (2006).
10. E. Schäffer, S. F. Nørrelykke, and J. Howard, "Surface forces and drag coefficients of microspheres near a plane surface measured with optical tweezers," Langmuir **23**, 3654–3665 (2007).
11. A. Rohrbach, "Stiffness of optical traps: Quantitative agreement between experiment and electromagnetic theory," Phys. Rev. Lett. **95**, 168,102 (2005).
12. A. Jannasch, V. Bormuth, C. Katz, A. van Blaaderen, J. Howard, and E. Schäffer, "Coated microspheres as enhanced probes for optical trapping," Proc. SPIE, submitted (2008).
13. G. Mie, "Articles on the optical characteristics of turbid tubes, especially colloidal metal solutions," Ann. Phys. **25**, 377–445 (1908).
14. T. A. Nieminen, V. L. Y. Loke, A. B. Stilgoe, G. Knoner, A. M. Branczyk, N. R. Heckenberg, and H. Rubinsztein-Dunlop, "Optical tweezers computational toolbox," J. Optic. Pure. Appl. Optic. **9**, S196–S203 (2007).
15. N. B. Viana, A. Mazolli, P. A. M. Neto, H. M. Nussenzveig, M. S. Rocha, and O. N. Mesquita, "Absolute calibration of optical tweezers," Appl. Phys. Lett. **88**, 131110 (2006).
16. G. Knoner, S. Parkin, T. A. Nieminen, N. R. Heckenberg, and H. Rubinsztein-Dunlop, "Measurement of the index of refraction of single microparticles," Phys. Rev. Lett. **97**, 157402 (2006).
17. N. B. Viana, M. S. Rocha, O. N. Mesquita, A. Mazolli, and P. A. M. Neto, "Characterization of objective transmittance for optical tweezers," Appl. Opt. **45**, 4263–4269 (2006).
18. M. D. Wang, H. Yin, R. Landick, J. Gelles, and S. M. Block, "Stretching DNA with optical tweezers," Biophys. J. **72**, 1335–1346 (1997).
19. S. B. Smith, Y. J. Cui, and C. Bustamante, "Overstretching B-DNA: The elastic response of individual double-stranded and single-stranded DNA molecules," Science **271**, 795–799 (1996).
20. J. Howard, A. J. Hudspeth, and R. D. Vale, "Movement of Microtubules by Single Kinesin Molecules," Nature **342**, 154–158 (1989).
21. C. Leduc, F. Ruhnow, J. Howard, and S. Diez, "Detection of fractional steps in cargo movement by the collective operation of kinesin-1 motors," Proc. Natl. Acad. Sci. U. S. A. **104**, 10847–10852 (2007).
22. Y. Hu, T. A. Nieminen, N. R. Heckenberg, and H. Rubinsztein-Dunlop, "Antireflection coating for improved optical trapping," J. Appl. Phys. **103**, 093119 (2008).
23. G. V. Shivashankar, G. Stolovitzky, and A. Libchaber, "Backscattering from a tethered bead as a probe of DNA flexibility," Appl. Phys. Lett. **73**, 291–293 (1998).
24. A. R. Clapp and R. B. Dickinson, "Direct measurement of static and dynamic forces between a colloidal particle and a flat surface using a single-beam gradient optical trap and evanescent wave light scattering," Langmuir **17**, 2182–2191 (2001).
25. D. L. J. Vossen, A. van der Horst, M. Dogterom, and A. van Blaaderen, "Optical tweezers and confocal microscopy for simultaneous three-dimensional manipulation and imaging in concentrated colloidal dispersions," Rev. Sci. Instrum. **75**, 2960–2970 (2004).
26. U. F. Keyser, B. N. Koeleman, S. Van Dorp, D. Krapf, R. M. M. Smeets, S. G. Lemay, N. H. Dekker, and C. Dekker, "Direct force measurements on DNA in a solid-state nanopore," Nature Phys. **2**, 473–477 (2006).
27. M. C. Noom, B. van den Broek, J. van Mameren, and G. J. L. Wuite, "Visualizing single DNA-bound proteins using DNA as a scanning probe," Nature Meth. **4**, 1031–1036 (2007).
28. C. Hertlein, L. Helden, A. Gambassi, S. Dietrich, and C. Bechinger, "Direct measurement of critical Casimir forces," Nature **451**, 172–175 (2008).
29. K. P. Velikov and A. van Blaaderen, "Synthesis and characterization of monodisperse core-shell colloidal spheres of zinc sulfide and silica," Langmuir **17**, 4779–4786 (2001).
30. V. Bormuth, J. Howard, and E. Schäffer, "LED illumination for video-enhanced DIC imaging of single microtubules," J. Microsc. **226**, 1–5 (2007).
31. J. B. Lamture, K. L. Beattie, B. E. Burke, M. D. Eggers, D. J. Ehrlich, R. Fowler, M. A. Hollis, B. B. Kosicki, R. K. Reich, S. R. Smith, R. S. Varma, and M. E. Hogan, "Direct-Detection of Nucleic-Acid Hybridization on the Surface of a Charge-Coupled-Device," Nucleic Acids Res. **22**, 2121–2125 (1994).
32. W. R. Schief, R. H. Clark, A. H. Crevenna, and J. Howard, "Inhibition of kinesin motility by ADP and phosphate supports a hand-over-hand mechanism," Proc. Natl. Acad. Sci. U. S. A. **101**, 1183–1188 (2004).
33. C. F. Bohren and D. R. Huffman, *Absorption and scattering of light by small particles* (Wiley, Weinheim, 2004).
34. S. N. S. Reihani and L. B. Oddershede, "Optimizing immersion media refractive index improves optical trapping by compensating spherical aberrations," Opt. Lett. **32**, 1998–2000 (2007).

1. Introduction

Optical tweezers are a sensitive position and force transducer widely employed in biophysics, colloid research, micro-rheology, and physics [1–7]. For many experiments, trapped

#96526 - $15.00 USD Received 27 May 2008; revised 24 Jul 2008; accepted 3 Aug 2008; published 22 Aug 2008

microspheres—so-called beads—are the object of interest or are used as handles for the measurements. In a high-numerical aperture focus, the beads can be stably trapped if for the axial direction the gradient force in the direction of highest light intensity is larger than the scattering force that pushes the particle away from the focus in the direction of light propagation. In a geometric optics picture, to first order, the scattering force is proportional to the reflectivity which scales with the square Δn^2 of the refractive index difference of the particle with respect to the surrounding medium. Due to Snell's law, the gradient force is to a first order approximation proportional to Δn. For a Rayleigh scatterer, the same scaling is true (see Appendix B). Thus, for high-refractive materials, the scattering force eventually dominates. This limits optical trapping.

Based on arguments from geometric optics, we hypothesized that using anti-reflection-coated microspheres would reduce scattering and lead to stronger trapping. Here, we designed, fabricated, and characterized polystyrene (PS) microspheres coated with silica (SiO_x) to test whether the trap stiffness of optical tweezers can be improved. We observed that in addition to an increased trap stiffness, the linear range of both the force gradient and the back focal plane positional detection was increased compared to uniform polystyrene spheres. Within the linear detection range, we achieved at least a $1.4\times$ higher trap force compared to any uniform polystyrene sphere. Moreover, we performed calculations of the trapping potential varying coating parameters, bead size, and materials. We found quantitative agreement of size and polarization dependence for coated and uncoated beads. Thus, we can use the theory to design core-shell particles to obtain the optimal trapping properties for an experiment, for example, microspheres having a high-refractive index core that cannot be trapped unless coated.

2. Results

2.1. Characterization

We coated PS microspheres ($n_{PS} = 1.57$) with SiO_x ($n_{SiO_x} = 1.45$) using the method of Graf *et al.* ([8] and see Methods). The refractive index of SiO_x nearly corresponds to the geometric mean of the indices from PS and water ($n_{H_2O} = 1.326$). Bright field, differential interference contrast, and transmission electron microscopy showed the smooth and homogeneous coating with an approximate thickness of 200 nm (middle row Fig. 1(b-e)). The coated beads crystalized for the electron microscopy measurements, indicating that they were monodisperse (see Table 1, Methods).

2.2. Trap stiffness

We measured the trap stiffness with which SiO_x, PS, and SiO_x-coated PS microspheres with a total diameter D ranging from $0.5\,\mu$m to $3\,\mu$m were held in an optical trap created with a linearly polarized (y-direction), $\lambda = 1064$ nm laser. All measurements were done in aqueous solutions close to a surface [Fig. 1(a)]. To calibrate position and force, we used our recently developed technique [9, 10] that is based on a drag force method using a small sinusoidal stage movement combined with power spectral analysis. This allowed us—without assumptions—to measure the diameter of the bead, its drag coefficient, the distance from the surface, and as a function of this microsphere-surface distance, the displacement sensitivity (the volt-to-meter conversion factor of the photodiode) and the trap stiffness for all spatial directions (see Methods). Foremost, we determined the lateral [Fig. 2(a)] and axial [Fig. 2(b)] trap stiffness at the surface for the three different bead types.

For both SiO_x and PS beads, there was a pronounced and sharp maximum in trap stiffness for beads with a diameter corresponding roughly to the trapping laser wavelength in the medium ($\approx 0.8\,\mu$m) [11]. Based on preliminary calculations (see Discussion and [12]), we did not expect to find improvements in trap stiffness for PS-SiO_x core-shell particles with a core diameter

#96526 - $15.00 USD Received 27 May 2008; revised 24 Jul 2008; accepted 3 Aug 2008; published 22 Aug 2008

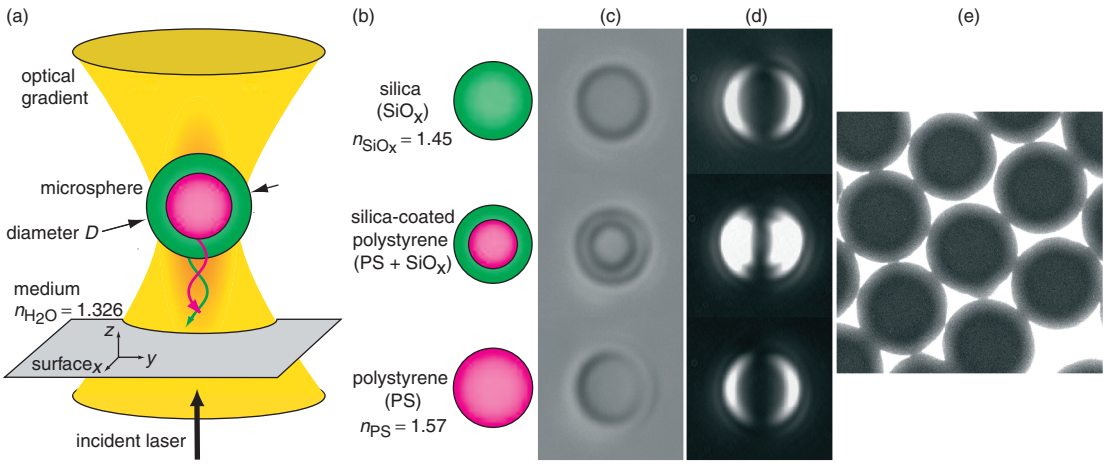

Fig. 1. (a) Setup geometry: A coated microsphere (bead) with diameter D is trapped in a tightly focussed, linearly polarized laser beam near a surface in an aqueous medium. The axial direction (propagation direction of the laser) is referred to as z. The laser is polarized in the y-direction. Light reflected back from the individual bead interfaces interferes and forms a standing light wave between the surface and the bead. (b) Schematic drawing of the silica (SiO_x, top), silica-coated polystyrene (PS+SiO_x, middle), and polystyrene (PS, bottom) microspheres. Refractive indices n are for a wavelength of 1064 nm. (c) Bright field and (d) differential interference contrast microscopy images of the respective microspheres in (b). (e) Transmission electron microscopy images of the coated microspheres. (c-e) Scale: All microspheres have an outer diameter of $\approx$1.5 μm.

of $\lesssim$0.8 μm. Therefore, we used core sizes of around 900 nm. The coated beads with a total diameter of 1.3 μm to 1.8 μm resulted in a more than two-fold stiffer trap compared to uniform PS and SiO_x beads of the same size. The trap stiffness depended only weakly on the coat-layer thickness. To mimic a microsphere with a very thick coating, denoted as $D = \infty$ in Fig. 2, we measured the trap stiffness of both the core alone and the core-shell bead in a solution that index-matched the shell (aqueous 80% by weight glycerol solution, $n = 1.45$). For the two bead types, we found the same trap stiffness that was, furthermore, comparable to the one of beads with a thin coating. Relative to the peak trap stiffness of PS, the coated beads were held with a $\approx$30% smaller trap stiffness. In contrast, compared to larger uniform microspheres the coated microspheres produced an up to 10-fold stiffer trap. In the axial direction, the coated beads had nearly the same trap stiffness compared to the maximum of the PS beads. All measurements, both in the lateral and axial directions, agreed quantitatively with Mie scattering calculations (see Theory and Methods).

2.3. Maximum restoring force

Coated beads experienced a higher maximal force in the trap than the core by itself. In Fig. 2(c), we have measured the maximal restoring force, also called the escape force, by moving the stage laterally with a constant applied acceleration relative to the trapped bead and recording the time from the start of the acceleration to the escape of the bead from the trap. The escape time determined the maximal drag force that could be balanced by the trap. The 1.5 μm-diameter coated beads had a $\approx$20% higher escape force compared to the core and a $\approx$60% higher ($\approx$15% lower) escape force compared to a SiO_x (PS) bead of the same diameter. Again, the measurements were in good agreement with Mie theory.

#96526 - $15.00 USD Received 27 May 2008; revised 24 Jul 2008; accepted 3 Aug 2008; published 22 Aug 2008

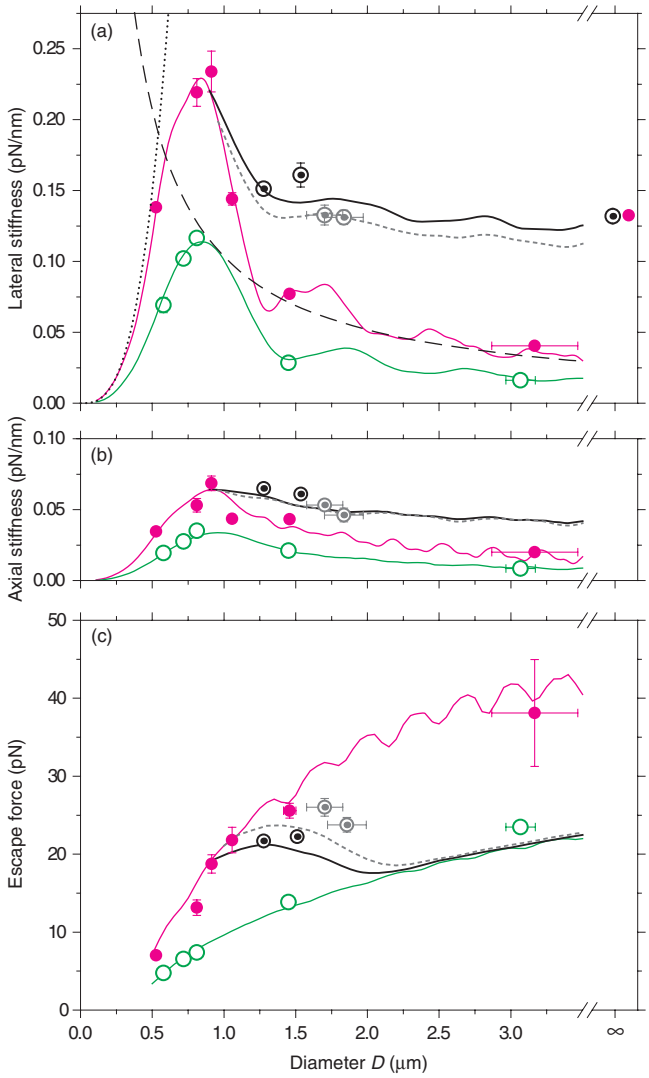

Fig. 2. (a) Lateral y, (b) axial z trap stiffness, and (c) lateral y escape force as a function of bead diameter for SiO_x (○), PS (●) and SiO_x-coated PS (⊙,⊙). The coated beads had two different cores: for $D \leq 1.5\,\mu$m the core diameter was 913 nm (⊙) and for $D > 1.5\,\mu$m the core size was 960 nm (⊙). The data points marked with ∞ were measured in a glycerol solution that index-matched the shell (see text). The symbols are averages ($N \gtrsim 6$) for each bead type. Errors are standard deviations and plotted if they were larger than the symbol size. Rayleigh (···, trap stiffness $\kappa \propto D^3$) and geometric optics (- - -, $\kappa \propto D^{-1}$) limits for PS. The other lines are Mie theory calculations. The laser power in (c) was 3× lower than in (a,b).

During the escape force measurements with a linearly increasing drag force, the detector response for the coated beads showed a linear increase up to nearly the point of escape (data not shown). The linear response corresponded to displacements of 360–470 nm depending on the coated bead size. For these displacements, the detector response for fixed bead scans was also still linear (see Sect. 2.4). Hence, the trap stiffness was constant up to these displacements.

#96526 - $15.00 USD Received 27 May 2008; revised 24 Jul 2008; accepted 3 Aug 2008; published 22 Aug 2008

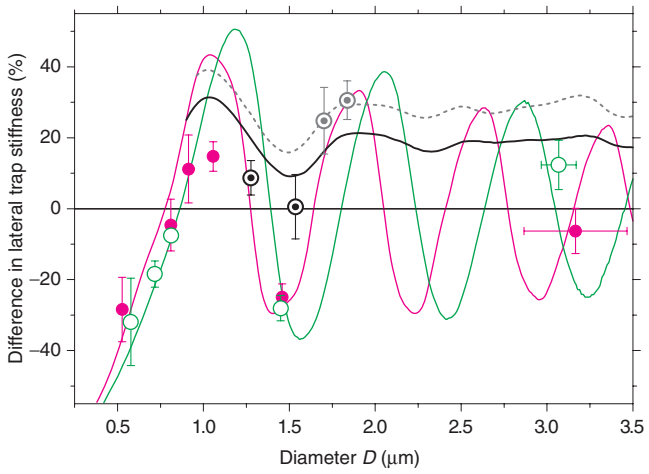

Fig. 3. Polarization dependence of the lateral trap stiffness as a function of bead diameter for SiO_x (○), PS (●) and SiO_x-coated PS (⊙,⊙). The plot shows the relative difference between the lateral trap stiffnesses $2(\kappa_y - \kappa_x)/(\kappa_x + \kappa_y)$. The laser was linearly polarized in the *y*-direction. The lines are the Mie theory results.

2.4. Practical issues

In addition to the trap stiffness and the maximal force, there are several other aspects that are of practical interest when working with optical tweezers. These include the effect of polarization on the trap stiffness, the linearity of the detection and force range, and the amount of backscattered light. Related to the last point are (i) the axial equilibrium position, i.e. how far the bead is pushed away from the laser focus and (ii) the amplitude of the standing light wave that forms between the bead and the surface [10].

Polarization. Based on our calculation, we observed that the differences in lateral trap stiffness changed signs several times depending on the size of the beads. We measured such sign changes, for example, twice for PS between 0.5 μm and 1.5 μm (Fig. 3) in agreement with the calculation. This means that depending on the size, the trap stiffness was either larger in the *x*- or in the *y*-direction. We measured differences up to ≈30%. Because the reflectivity generally depends on the polarization, these observations are consistent with the trap stiffness being dependent on the polarization of the laser. The change of signs implies that there are cross-over points where the *x* and *y* trap stiffnesses are equal. This was also borne out by the theory.

Linearity. We measured the detector response and found an increased linear range for the 1.5 μm-diameter coated particles compared to the uniform beads. To measure the response, we scanned fixed beads through the laser by moving the stage laterally. The resulting detector signal as a function of stage position is plotted in Fig. 4(a). The slope of this signal corresponds to the inverse of the displacement sensitivity at the surface. Compared to the 1.5 μm-diameter uncoated beads, the detector response for the coated particles showed that the gradient in the center was not only the highest but also remained nearly constant over a more than 2.5-fold larger region ($\pm$500 nm with $\leq$10% deviation). In particular, the curve did not show points of inflection at the extent of the lateral laser focus ($\approx \pm 0.4\,\mu$m). Compared to the smaller 0.9 μm-diameter uncoated beads, the linear range was also 2.5-fold larger. In addition to the detector response, we calculated the trapping force as a function of bead displacement from the center. The curves resembled in shape those of Fig. 4(a) (data not shown, [12]). We confirmed the con-

#96526 - $15.00 USD Received 27 May 2008; revised 24 Jul 2008; accepted 3 Aug 2008; published 22 Aug 2008

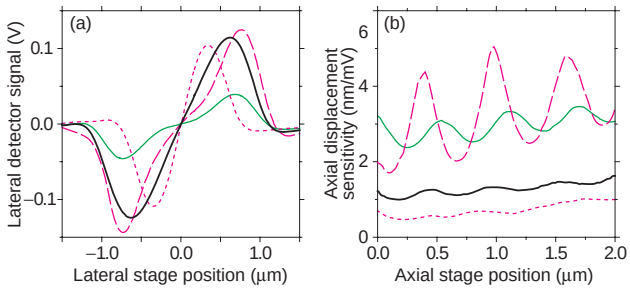

Fig. 4. (a) Lateral detector signal measured as a function of lateral stage position for surface-immobilized beads. (b) Axial displacement sensitivity as a function of stage height for the three different bead types using the same laser intensity. At stage height zero, microspheres touch the surface. The displacement sensitivity increases linearly with distance to the surface due to spherical aberrations [10]. Oscillations are due to a standing light wave between the surface and the bead. (a,b) 1.5 μm-diameter bead: — PS+SiO_x, — SiO_x, – – PS; 0.9 μm-diameter bead: - - - PS.

stancy in trap stiffness experimentally by our drag/escape force measurements (see Sect. 2.3) and by using the well-characterized, force-induced melting transition of DNA as a calibration standard (see Sect. 4). Therefore, also the force response of the coated particles had a larger linear range compared to the uniform beads. How large the linear range is depends in a non-trivial manner on the parameters of the system. It therefore needs to be measured or calculated. Generally, in particular for large core sizes, the linear range of the coated beads might not be significantly larger compared to uniform microspheres.

Backscattered light. When working close to a surface, backscattered light from the bead forms a standing light wave between the bead and the surface [7, 10]. Since we intended to reduce the amount of backscattering by the coating, we expected that the amplitudes of these oscillations would be reduced. Previously [10], we reported small oscillations in the lateral displacement sensitivity and the total laser intensity at the detector. Here, we show that the axial displacement sensitivity was modulated up to 50% in amplitude for the high-refractive 1.5 μm-diameter PS beads [Fig. 4(b)]. In contrast, both the silica and coated spheres scattered back less light and, therefore, only showed a minor modulation.

3. Theory

Since the size of particles that are typically used for optical trapping falls in the range where Rayleigh scattering and geometric optics are not applicable, computational approaches are necessary to quantitatively calculate the trapping efficiency. Most pertinent for optical tweezers is the theory based on Mie's now 100 year old classic paper [13]. This exact theory was recently implemented using the $\boldsymbol{T}$-matrix method in an optical tweezers computational toolbox [14], written in MATLAB®, that we extended in the current work to include coated spheres (see Methods). Several studies demonstrated quantitative agreement between theory and experiment for uniform microspheres, however, with limited ranges of bead diameters [11, 15, 16].

Compared to these studies, we have quantitative agreement for different materials and bead sizes covering both the Rayleigh and geometric optics limits. The lines in Figs. 2,3,6 are the best fit of the Mie theory to all trap stiffness measurements of SiO_x and PS. The best fit was obtained with respect to the following parameters: the refractive indices of the particles ($n_{SiO_x} = 1.45$, $n_{PS} = 1.57$), the effective numerical aperture ($NA_{eff} = 1.25$), the amount of overfilling described by a truncation angle ($\theta = 71^\circ$ corresponding to $\omega/a = 0.9$ filling of the objective

#96526 - $15.00 USD Received 27 May 2008; revised 24 Jul 2008; accepted 3 Aug 2008; published 22 Aug 2008

back aperture having a radius a with respect to the Gaussian beam waist ω consistent with our setup), and the laser power (e.g. in Fig. 2(a,b) the calculated power in the focus was 62 mW). No other adjustable parameters entered. The effective numerical aperture is lower than the NA $= 1.3$ specification for the trapping objective. We think that the reduction is mostly caused by a smaller transmission of the objective at the outer edges for the incoming beam [17]. The magnitude of the reduction is similar to that reported in [17]. Other factors that contributed to a lower effective NA were the non-ideal Gaussian laser beam and deficiencies in the theory such as a phenomenological description of the effect of overfilling and a lack of treatment of spherical aberrations. These factors may also explain discrepancies between individual data points and the theory. In addition, beads from individual batches may have different refractive indices or be slightly elliptical in shape.

The relative root-mean-squared deviation of the data from the theory was 10%. This quantitative agreement implies that a force calibration is unnecessary if our achieved accuracy is sufficient and/or calibration procedures are difficult, for example, when working inside cells. Furthermore, it lends trust to the calculations that the theory and computations can be used to design optimal-coated microspheres.

4. DNA and kinesin assay

To demonstrate the use of the coated microspheres in biophysical experiments, we designed an experiment to probe the collective behavior of kinesin motors under forces up to 100 pN (Fig. 5). The assay is facilitated by using the coated beads since it can be done with a relatively low-power laser. For our maximal laser intensity, large displacements were necessary to reach a force of 100 pN. To confirm the linear range of the force gradient for such large displacements in addition to our drag force measurements (see Sect. 2.4), we measured a DNA force-extension curve [Fig. 5(c)]. We chose a low laser intensity (0.46 W laser output) such that the displacements from the trap center reached values of close to 300 nm. In this manner, we measured $\approx$62 pN for the force-induced melting plateau. Since this value is in good agreement with literature values [6, 18, 19], the linear detection and force range must be at least 300 nm, which is about 2.5-fold higher than reported in [18]. This large linear range enabled us to measure the high forces generated by large numbers of motor proteins. A coated microsphere was attached to a microtubule through a biotin-NeutrAvidin linkage (see Methods). Such microtubules were allowed to glide over a surface coated with a high density of the motor protein kinesin-1 in which $>$10 motors moved each microtubule [20]. The motors were able to displace the microsphere up to 300 nm from the trap center with corresponding forces of 100 pN. No discrete 8-nm steps were visible over the entire force range (an exemplary region is shown in Fig. 5(b)). This shows that the motors were not synchronized (i.e. they did not take 8-nm steps in unison). With much better resolution, this finding is in agreement with a recent study revealing that the step size is divided down by the number of participating motor proteins [21]. Furthermore, our measurements show that multiple motors can produce high forces (much greater than the single-motor force). Large backward movements (e.g. at 5.5 and 12.5 s) are due to bead detachment/reattachment from and to the microtubule by disruption/binding of the biotin-NeutrAvidin linkages, as confirmed by control experiments (data not shown, see Methods).

5. Discussion

Anti-reflection. We set out to reduce the amount of backscattering on microspheres trapped in optical tweezers. Surprisingly, we found that already an uncoated bead with the correct size acts effectively as a perfect anti-reflection coated particle (0.9 μm PS bead in Fig. 4(b)). This is due to the destructive interference of light reflected from the upper and lower bead-medium interface (see Appendix A). Since a particle that scatters back less light is situated closer to the focus

#96526 - $15.00 USD Received 27 May 2008; revised 24 Jul 2008; accepted 3 Aug 2008; published 22 Aug 2008

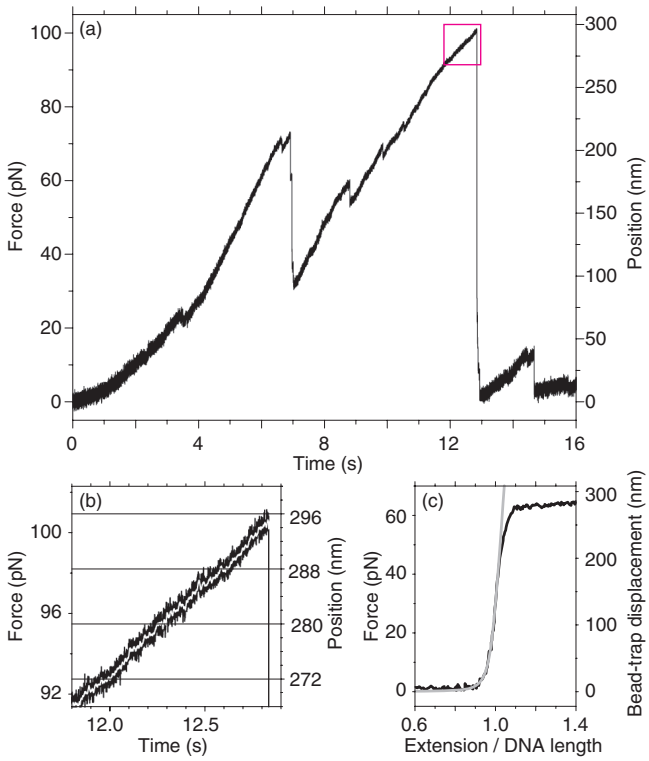

Fig. 5. (a) High-force kinesin-1 motor protein assay. A NeutrAvidin modified coated microsphere was attached to a biotinylated microtubule transported by multiple motors that are attached to the coverslip surface (10 μM ATP, see Methods). The magenta rectangle indicates the region that is displayed in (b) with a higher magnification. (b) Close-up view of the region marked in (a). No steps are discernable. (c) DNA force-extension curve. A 1 μm-long DNA (—) was pulled laterally (see Methods and [18]). An extensible worm-like chain model (—) describes the data well. (a-c) We used 1.5 μm-diameter coated beads (PS+SiO_x).

(Fig. 6), non-linearities and usually unwanted oscillations in calibration parameters [Fig. 4(b)], in particular in the axial direction, are reduced. For the coated beads, the overall amount of backscattered light is reduced compared to the PS core. The lowest amount of backscattering is achieved with the 1.3 μm-diameter, coated beads. These beads have a silica layer thickness that corresponds to the optimal coating for a planar anti-reflection coating (see Appendix A). Furthermore, based on our calculations (data not shown, [22]), since less light is scattered back trapping is possible with a lower-NA objective or underfilling of the trapping objective. Thus, cheaper low-NA objectives with a larger working distance can be used for trapping.

Index matching. With increasing shell thickness, the coated particle's trap stiffness rapidly approached a more or less constant value. Surprisingly, there was little difference between a 200 nm- and an ∞-thick coating. In addition, the trap stiffness did not approach the one of silica—for example, for a total diameter of 3.5 μm, the PS core has a volume of less than 2% compared to the total. At that diameter, the coated bead trap stiffness is $\approx 10\times$ higher compared to SiO_x beads of the same size. This can be understood by our index-matching experiment (∞-data point in Fig. 2): If the shell has the same refractive index as the surrounding medium the trapping strength is completely independent of the shell thickness since light is not refracted at

#96526 - $15.00 USD Received 27 May 2008; revised 24 Jul 2008; accepted 3 Aug 2008; published 22 Aug 2008

the medium-shell interface. Hence, there is no change in light momentum attributed to the shell. The same must nearly be true for the coated beads with a 200 nm-thick shell in water, since their trap stiffness was comparable to the index matched measurement. This means that the scattering from a core-shell particle is similar to that of a core-sized uniform bead alone having the same reduced relative refractive index ($n_{\mathrm{uniform}}/n_{\mathrm{medium}} = n_{\mathrm{core}}/n_{\mathrm{shell}}$). Thus, a 0.9 μm-diameter microsphere with the refractive index of $n_{\mathrm{uniform}} = n_{\mathrm{medium}} n_{\mathrm{core}}/n_{\mathrm{shell}} \approx 1.446$ in water would have about the trap stiffness of our 0.9 μm-core diameter, SiO_x-coated beads.

Trap stiffness and maximal forces. The choice of microsphere is determined by the requirements of the experiment. The highest trap stiffness is not always the only consideration. For instance, to resolve fast dynamics in motor protein studies, beads with a low drag coefficient and thus with a small diameter (< 800 nm) are used. For various reasons, for instance to reduce the light intensity at the surface where the protein of interest is adsorbed, larger microspheres are used in many studies (e.g. 1.4-4 μm diameter in [19, 23–28]). Therefore, for such large beads, it would be very useful to be able to attain high trapping stiffnesses with less laser power. In this size range, our coated microspheres provide a substantial improvement compared to beads with at least the same outer diameter. For the 1.5 μm-diameter coated beads (trap stiffness $\kappa_y = 0.16$ pN/nm, Fig. 2(a)), we measured a 10-fold increase in trap stiffness compared to the 3.1 μm-diameter silica beads ($\kappa_y = 0.016$ pN/nm, Fig. 2(a)). Since the trap stiffness of the coated beads remained nearly constant for increasing coat thickness (∞-data point in Fig. 2) and the trap stiffness of uniform beads decreased proportional to D^{-1}, the improvement factor in trap stiffness of our coated beads scaled directly with the bead diameter D. Even compared to the 0.9 μm-diameter PS beads that had the highest trap stiffness, the highest forces in the linear operating range of the tweezers were still achieved with the coated beads. With a $>2\times$ larger linear range for the coated beads [Fig. 4(a)] and $\approx 0.7\times$ of the maximal trap stiffness [Fig. 2(a)], the maximal force—for a Hookean spring the displacement times the trap stiffness—was $\gtrsim 1.4\times$ larger for the coated compared to the optimal trap stiffness, 0.9 μm-diameter, PS beads. This was advantageous for the high-force motor protein assay (Fig. 5). The trade-off is a lower bandwidth due to the larger drag coefficient of the coated beads compared to the 0.9 μm-diameter PS beads.

Achieving ultimately even higher trap efficiencies also for smaller beads is only possible for higher refractive index materials. However, there is an upper limit for the refractive index for which uniform microspheres can still be trapped (see Introduction and Appendix B). Coating high-n particles, opens up new possibilities to trap for instance particles with a ZnS [29] or TiO_2 ($n \approx 2.4$) core in a single beam tweezers. For such high-n cores, coated particles with an overall diameter $D \approx \lambda$ can be realized with a higher trapping efficiency than PS. For the parameters of our setup, if we use an optimal coated TiO_2-core microsphere with an outer diameter of ≈ 1 μm, theoretically having 4 W of laser power, we could achieve a trap stiffness of 4.3 pN/nm (≈ 7.4 pN/(nm W); more than 2-fold larger compared to PS). Thus, with a displacement of 240 nm, which is still well within the linear detection range for the coated particles, a force of more than 1 nN could be realized. Experiments in the nanonewton force range, for instance protein unfolding or intra- and intercellular measurements, with at least a nanonewton resolution are therefore feasible.

6. Methods

6.1. Microsphere coating

Based on geometric optics, the ideal anti-reflection coating for PS ($n_{\mathrm{PS}} = 1.57$) in water ($n_{H_2O} = 1.326$) is a layer with a refractive index of $n_{\mathrm{shell}} = 1.443$ and a thickness of 184 nm for a wavelength of $\lambda = 1064$ nm. Therefore, we chose silica ($n_{SiO_x} = 1.45$) as coating material.

To coat PS microspheres with a comparatively thick layer of silica, we extended estab-

#96526 - $15.00 USD Received 27 May 2008; revised 24 Jul 2008; accepted 3 Aug 2008; published 22 Aug 2008

Table 1. Specifications for the coated microspheres: mean±standard deviation in μm (polydispersity[a] in %, number of measurements N if known). The total diameter D was measured with transmission electron microscopy (TEM) and our optical tweezers calibration method.

PS core diameter[b]	SiO_x shell thickness[c]	Total diameter: TEM	Optical tweezers
0.91 ± 0.03 (2.6)	0.19 ± 0.01 (3.5, 7)	1.34 ± 0.04 (2.8, 25)	1.28 ± 0.03 (2.3, 7)
0.91 ± 0.03 (2.6)	0.31 ± 0.01 (3.7, 7)	1.55 ± 0.04 (2.5, 100)	1.53 ± 0.04 (2.6, 7)
0.99 ± 0.1 (10)	0.37 ± 0.03 (7.2, 6)	1.54 ± 0.08 (5.1, 30)	1.70 ± 0.12 (7.1, 6)
0.99 ± 0.1 (10)	0.42 ± 0.03 (7.7, 6)	1.76 ± 0.12 (6.6, 20)	1.84 ± 0.14 (7.6, 6)

[a] The polydispersity is defined here as the coefficient of variation (standard deviation divided by mean).
[b] Specification from supplier. For the larger core, control measurements with TEM resulted in 0.96 ± 0.01 (1.1, 26).
[c] The shell thickness is based on the difference between core and total diameter (optical tweezers measurements). Errors are propagated.

lished procedures [8]. As a core, we used either positively charged, amine functionalized PS microspheres with a diameter of 913 ± 24 nm (Polysciences, Warrington, USA) or non-functionalized 0.96 μm PS spheres (Bangs Laboratories, Fishers, USA). The beads were first cleaned in water. Only the non-functionalized beads were treated with a 0.07 wt.% poly(allylamine hydrochloride) solution containing 0.36 M NaCl. Both types of PS beads were then coated with a monolayer of the amphiphilic, non-ionic polymer poly(vinylpyrrolidone) (PVP, Sigma Aldrich) with an average molar mass of 360 kg/mol in an ethanol solution. To the ethanol solution containing the PVP-stabilized particles, we then added an ammonia solution and subsequently a tetraethoxysilane solution (0.1 M) in a stepwise manner while stirring. The concentration, volume, and number of steps ($\leq$5) determined the final coating thickness. We separated products from secondary nucleation by centrifugation. The procedure was robust to produce silica layers of up to at least 420 nm thickness. Sizes for the coated microspheres used in this study are given in Table 1.

6.2. Optical tweezers

The setup was essentially the same as in [10, 30] except for an added Faraday isolator (IO-3-1064-VHP, Optics for Research, Caldwell, USA) directly after the laser head and before the first beam expander. Briefly, a 1.5 W Nd:YVO_4 laser ($\lambda = 1064$ nm, M^2-value of $\approx$1.25, Smart Laser Systems, Berlin, Germany) was expanded to a beam waist of $\omega \approx 2.8$ mm and coupled into an inverted microscope. The trapping objective was a Zeiss Plan-Neofluar 100×, 1.3 NA, oil-immersion objective with a back aperture radius of $a \approx 6$ mm. We used a position-sensitive photodiode for back-focal-plane detection in three dimensions.

6.3. Sample preparation & calibration

For comparison, we used 0.5–3 μm-diameter PS and SiO_x microspheres (Polysciences, Warrington, USA and Bangs Laboratories, Fishers, USA). Bead cleaning and flow cell construction were the same as in [10]. Flow-cells with a 3 mm-wide channel consist of one $18 \times 18\,mm^2$ coverslip on top of a $22 \times 22\,mm^2$ coverslip separated by a $\approx$100 μm-thick layer of parafilm. The cleaned coverslips were not treated further. We then filled the channels with the solution of interest containing the microspheres. All measurements were done in a 50 mM KCl solution at room temperature (sample temperature measured at $26.5 \pm 0.1\,^{\circ}C$) with the same laser intensity unless otherwise noted.

For each bead type, we acquired data for at least 6 beads and for each individual bead power spectra in x, y, and z at $\approx$100 positions covering bead-surface separations of zero to $\approx 3\,\mu$m

#96526 - $15.00 USD Received 27 May 2008; revised 24 Jul 2008; accepted 3 Aug 2008; published 22 Aug 2008

(4.5 μm) for beads with $D \leq 1\,\mu$m ($D > 1\,\mu$m). We analyzed the raw data as a function of bead-surface distance by an automated, global fitting routine [10]. Since for every position we measured independently the trap stiffness, the displacement sensitivity, and the drag coefficient, we could rule out artifacts arising from assumptions about the microsphere size and the distance to the surface concurrent with the dependence of the drag coefficient on this distance (e.g. Faxén's law, see [10]).

6.4. DNA & kinesin assay

The 3133 bp DNA was produced with PCR utilizing 5' amino- and 5' biotin-modified primers. The amino-modification was used to covalently attach the DNA to the surface [31] and the biotin to bind the NeutrAvidin-modified microspheres (see below). Experiments were done in 20 mM Tris-HCl, pH 7.5, 10 mM NaCl, and 0.1% Tween 20. To stretch the DNA, the piezo translation stage was moved in a sinusoidal fashion with an amplitude of 1.5 μm at a frequency of 1 Hz. Stable microtubules were grown by incubating 2 μM biotinylated tubulin (Cytoskeleton, Denver) and 1 mM GMP-CPP (Jena Bioscience, Jena, Germany) in BRB80 [21] with 1 mM $MgCl_2$ at 37 °C for 3 hours. The microtubules were cleaned by centrifugation in BRB80 with 10 μM paclitaxel (Sigma). Gliding motility was prepared as in [32]. SiO_x-coated microspheres were passively functionalized by incubating them in 1 mg/ml NeutrAvidin (Pierce, Rockford, USA) solution in PBS for 30 min. at 25 °C and 4 hours at 4 °C. Beads were cleaned by centrifugation. Control experiments were done in AMPPNP by moving the stage laterally in 8 nm steps to simulate motor activity. Since in AMPPNP motors are bound stationary to the microtubule, we attributed large sudden movements to a detachment of the beads from the microtubule.

6.5. Scattering theory

We used and extended the optical tweezers computational toolbox of Nieminen *et al.* [14] to calculate the trapping parameters for homogeneous and coated microspheres. Recently, the authors of the toolbox also extended it to include coated spheres [22]. Their calculations are in agreement with our calculations and experiments. In short, the electric field of the incoming light, a Gaussian beam, is described by a discrete orthogonal set of functions that are a solution to the vector Helmholz equation. The scattered light is expanded in the same basis leading to a linear relationship between the incident and scattered field. Consequently, the expansion coefficients are related by a matrix. For a homogeneous isotropic sphere, this so-called $\boldsymbol{T}$-matrix is diagonal and its elements are the coefficients of Mie's analytical solution [13]. An analytical solution also exists for a core-shell particle with a homogeneous concentric shell [33]. The $\boldsymbol{T}$-matrix is independent of the position and illumination of the particle and must only be calculated once. This makes the method efficient. Finally, the imparted force on the sphere is calculated by integrating the Maxwell stress tensor over a surface encompassing the latter. Included in the calculation is that the Gaussian beam is cut off by the entrance aperture of the objective. Absent is a treatment of spherical aberrations occurring at a glass-water interface when using oil immersion objectives, which in experiments can be influenced by changing the refractive index of the immersion oil or using a non-parallel laser beam [34].

Acknowledgments

We thank Dirk Vossen for early calculations on the scattering of coated microspheres, Henning Urban for early work on the DNA assay, Timo A. Nieminen and Halina Rubinsztein-Dunlop for an early version of the optical tweezers computational toolbox, and Simon Nørrelykke and Stephan Grill for comments on the manuscript. The work was supported by the Deutsche Forschungsgemeinschaft (Emmy Noether Program), the Max Planck Society, and the Technische Universität Dresden. Patent application pending.

#96526 - $15.00 USD Received 27 May 2008; revised 24 Jul 2008; accepted 3 Aug 2008; published 22 Aug 2008

Author contributions

E.S. designed research; V.B., A.J., M.A., C.M.v.K., and E.S. performed research; C.M.v.K. and A.v.B. contributed new reagents/analytic tools; A.J., V.B., M.A. and E.S. analyzed data; A.v.B. and J.H. provided advice and commented on the manuscript; and E.S. wrote the paper.

Appendix A: Anti-reflection

Since the scattering force acts only in the direction of light propagation, we expected that its reduction results in a stable axial trapping position closer to the laser focus. In addition, for a reduced amount of backscattered light, we also expected that the amplitude of the standing light wave between the surface and the bead was reduced. This standing light wave modulated both the displacement sensitivity [Fig. 4(b)] and the laser intensity recorded on the photodiode [7]. We measured the oscillation amplitudes of this laser intensity for the three different bead types as a function of diameter (symbols in Fig. 6, right-hand scale).

Anti-reflection coated beads with a quarter-wave shell thickness ($\approx$1.3 μm outer diameter) showed the least amount of backscattering compared to all measured beads (Fig. 6). Intriguingly, these amplitudes scaled roughly with the calculated, axial equilibrium position (lines in Fig.6, left-hand scale). For the coated particles, this equilibrium position was on average closer to the focus compared to the uniform beads. In addition, for all beads there was a modulation of the equilibrium axial trapping position with size. These oscillations are a manifestation of the interference of the light scattered back from the upper and lower interfaces of the bead. For increasing outer diameter D, the periodicity of the oscillations approached exactly a multiple of half a wavelength inside the bead (inset of Fig. 6). Thus, the phase shift of light rays reflected from the top and bottom of a bead is $(\ell + \frac{1}{2})\lambda$ where ℓ is an integer. This includes the $\lambda/2$ phase shift at the reflection of the optical not-so-dense to the dense medium, i.e. at the bottom water-bead interface. The total phase shift thus leads to destructive interference. This interference explains why the uncoated 0.9 μm-diameter bead behaved effectively as a perfect anti-reflection coated particle.

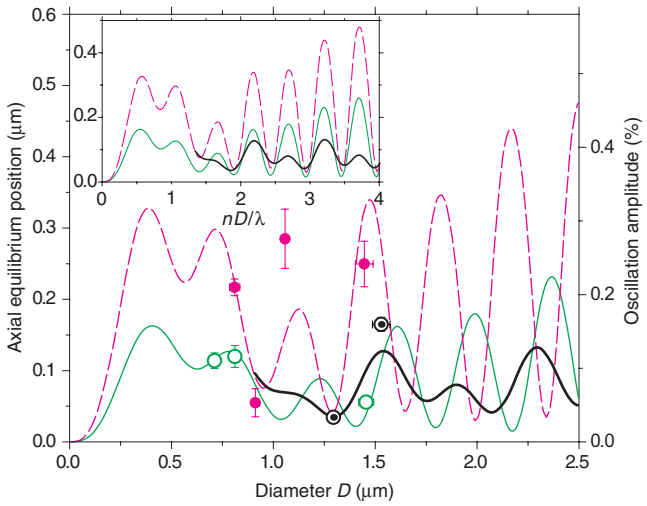

Fig. 6. Axial equilibrium position (— PS+SiO_x, — SiO_x, – – PS; left-hand scale) and normalized oscillation amplitude of laser intensity (○ SiO_x, ● PS, ⊙ SiO_x+PS; right-hand scale) as a function of bead diameter D. The inset shows the equilibrium position with a rescaled abscissa: the diameter in units of the laser wavelength inside the bead.

#96526 - $15.00 USD Received 27 May 2008; revised 24 Jul 2008; accepted 3 Aug 2008; published 22 Aug 2008

Appendix B: Scaling of the trapping forces with the refractive index difference Δn

Rayleigh regime. The scattering force is given by [1]

$$F_{\text{scat}} = n_{\text{medium}} \frac{\langle S \rangle \sigma}{c} \tag{1}$$

in terms of the time-averaged Poynting vector $\langle S \rangle$, the speed of light c, and the scattering cross section

$$\sigma = \frac{2}{3}\pi^5 \left(\frac{n_{\text{medium}}}{\lambda}\right)^4 D^6 \left(\frac{m^2-1}{m^2+2}\right)^2 \tag{2}$$

where $m = n_{\text{bead}}/n_{\text{medium}}$. The term involving the refractive indices is

$$\frac{m^2-1}{m^2+2} = \frac{n_{\text{bead}}^2 - n_{\text{medium}}^2}{n_{\text{bead}}^2 + 2n_{\text{medium}}^2} = \frac{(n_{\text{bead}} - n_{\text{medium}})(n_{\text{bead}} + n_{\text{medium}})}{n_{\text{bead}}^2 + 2n_{\text{medium}}^2} \propto \Delta n \tag{3}$$

where $\Delta n = n_{\text{bead}} - n_{\text{medium}}$. Thus,

$$F_{\text{scat}} \propto \Delta n^2. \tag{4}$$

The gradient force is given by

$$F_{\text{grad}} = \frac{\alpha}{2} \nabla \langle E^2 \rangle \tag{5}$$

with the polarizability

$$\alpha = \frac{1}{8} n_{\text{medium}} D^3 \left(\frac{m^2-1}{m^2+2}\right). \tag{6}$$

Thus,

$$F_{\text{grad}} \propto \Delta n. \tag{7}$$

Geometric optics regime. In the geometric optics limit ($D \gg \lambda$), we assume a small—compared to the diameter—bead displacement out of the focus in the axial direction. Furthermore, we neglect interferences and multiple reflections. Under these assumptions, all light rays hit the microsphere under nearly normal incidence. Thus, we can use small angle approximations ($\sin\theta \approx \theta$ and $\cos\theta \approx 1$). In the following we consider the reflection and refraction of a single light ray incident at an angle θ_1 with respect to the normal of the microsphere surface. For $\theta_1 \ll 1$, the reflected light ray exerts a scattering force proportional to the reflectivity

$$F_{\text{scat}} \propto \left(\frac{n_{\text{bead}} - n_{\text{medium}}}{n_{\text{bead}} + n_{\text{medium}}}\right)^2 \propto \Delta n^2. \tag{8}$$

The refracted ray changes direction according to Snell's law

$$\theta_1 n_{\text{medium}} = \theta_2 n_{\text{bead}}. \tag{9}$$

A change in the direction of the light ray leads to a momentum transfer from the light ray to the microsphere resulting when summed up to the gradient force. For a single ray, with a transmission close to 1, passing through the bead

$$F_{\text{grad}} \propto 2\sin(\theta_1 - \theta_2) \approx 2(\theta_1 - \theta_2) = \frac{2\theta_1}{n_{\text{bead}}}(n_{\text{bead}} - n_{\text{medium}}) \propto \Delta n. \tag{10}$$

Summing over all light rays preserves the scaling.

#96526 - $15.00 USD Received 27 May 2008; revised 24 Jul 2008; accepted 3 Aug 2008; published 22 Aug 2008